Cell Host & Microbe
Article

Genome-wide Analysis of Heterochromatin Associates Clonally Variant Gene Regulation with Perinuclear Repressive Centers in Malaria Parasites

Jose-Juan Lopez-Rubio,[1,2] Liliana Mancio-Silva,[1,2] and Artur Scherf[1,*]
[1]Unité de Biologie des Interactions Hôte-Parasite, CNRS URA2581, Institut Pasteur, 25 Rue du Dr. Roux, 75724 Paris, France
[2]These authors contributed equally to this work
*Correspondence: artur.scherf@pasteur.fr
DOI 10.1016/j.chom.2008.12.012

SUMMARY

Clonally variant gene families underlie phenotypic plasticity in *Plasmodium falciparum*, a process indispensable for survival of the pathogen in its human host. Differential transcription of one of these gene families in clonal parasite lineages has been associated with chromatin modifications. Here, we determine the genome-wide distribution in *P. falciparum* of a histone mark of heterochromatin, trimethylation of histone H3 lysine 9 (H3K9me3), using high-resolution ChIP-chip analysis. We show that H3K9me3 is specifically associated with clonally variant gene families, which are clustered on subtelomeric and some chromosome internal regions. High levels of H3K9me3 correlate with genes localized to the nuclear periphery, implying chromosome loop formation. Disruption of the histone deacetylase PfSir2 causes changes in H3K9me3 that are discontinuous along chromosomes and associated with disrupted monoallelic transcription. Our data point to the existence of perinuclear repressive centers associated with control of expression of malaria parasite genes involved in phenotypic variation and pathogenesis.

INTRODUCTION

The human protozoan malaria parasite *P. falciparum* kills more than 2 million people (mainly children) per year (Snow et al., 2005). This parasite is well adapted to survive in changing host environments such as the *Anopheles* mosquito midgut and salivary glands, human liver hepatocytes, and erythrocytes. Malaria pathogenesis is linked to the parasite's capacity to develop different phenotypic states in genetically clonal blood stage parasites (Fried and Duffy, 1996; Jensen et al., 2004). However, most processes causing pathogenesis are not yet understood at the molecular level and may involve expression of particular combinations of clonally variant molecules.

In *P. falciparum*, phenotypic diversity is commonly achieved by the expression of clonally variant surface molecules either at the erythrocyte membrane or merozoite surface (Cortes et al., 2007; Scherf et al., 1998; Stubbs et al., 2005). Switching of expression to another variant molecule prolongs the period of infection and generates alternative evasion pathways. Little is known about factors that govern phenotypic plasticity. The best-studied example of variant surface proteins is the *P. falciparum* erythrocyte membrane protein 1 (PfEMP1) (Leech et al., 1984). PfEMP1 is a major virulence factor involved in antigenic variation and adherence of infected erythrocytes to host receptors, resulting in their sequestration to capillaries in the brain and other critical organs (Kyes et al., 2007). PfEMP1 is encoded by genes of the 60 member *var* family, which are located on subtelomeric and internal chromosome loci. In a single parasite, only one *var* gene is expressed in a mutually exclusive manner under the control of epigenetic factors (Scherf et al., 1998).

A number of recent publications point to reversible chromatin changes, such as histone methylation and acetylation, as important control elements of *P. falciparum* gene silencing and monoallelic activation (reviewed in Scherf et al., 2008a). Enzymes that add or remove acetyl and methyl marks in *P. falciparum* have also been identified (Cui et al., 2008; Merrick and Duraisingh, 2007; Miao et al., 2006). It has been demonstrated that trimethylation of histone H3 lysine 9 (H3K9me3) is associated to transcriptionally silent *var* genes (Chookajorn et al., 2007; Lopez-Rubio et al., 2007). Upon *var* gene activation, in the 5′ flanking region (5′UTR), methylation is replaced by acetylation at lysine 9 of histone H3 (H3K9ac), and histone H3 lysine 4 is di- and trimethylated (H3K4me2/3) (Lopez-Rubio et al., 2007). Furthermore, PfSir2 histone deacetylase has been shown to spread from telomeres into the subtelomeric coding regions, leading to stable but reversible repression of subtelomeric *var* genes (Duraisingh et al., 2005; Freitas-Junior et al., 2005; Mancio-Silva et al., 2008). Genetic elements such as the 5′UTR (Voss et al., 2006) contain essential information able to interact with the epigenetic control machinery. Experimental data suggest that the *var* intron-linked promoter activity also contributes to monoallelic expression (Dzikowski et al., 2006).

Sequencing of the *P. falciparum* genome has led to the discovery of multiple gene families mainly clustered at subtelomeres adjacent to *var* genes (Gardner et al., 2002). A few of these have been studied, such as *rif* (Fernandez et al., 1999; Kyes et al., 1999), *clag* (Cortes et al., 2007), *stevor*, and *PfMC-2TM* (Blythe et al., 2008; Lavazec et al., 2007) and, similarly to *var* genes, are clonally variant and possibly involved in immune evasion (Scherf et al., 2008a). Telomeres are spatially restricted to nuclear periphery, where they form clusters of three to seven

heterologous chromosome ends (Freitas-Junior et al., 2000). This compartment is believed to enhance continual genetic exchange between members of gene families and may explain the vast *var* repertoire diversity observed between field isolates (Barry et al., 2007). Investigating the role of clusters in gene expression has resulted in inconsistent data. Experimental evidence, using parasites transfected with various constructs, reported relocation of an active *var* gene into a cluster (Duraisingh et al., 2005; Marty et al., 2006; Voss et al., 2006), whereas other studies, using parasite populations expressing a single *var* gene, observed the relocation outside of cluster (Ralph et al., 2005).

Whether phenotypic variation shares common epigenetic control mechanisms in any pathogenic parasite remains unclear. Here, we report that repressive centers at the perinuclear space participate in virulence gene family silencing in *P. falciparum*. Genome-wide analysis of histone modifications revealed that heterochromatic mark H3K9me3 is restricted to clonally variant gene families. Furthermore, we demonstrate that H3K9me3 is associated to the perinuclear location of internal and subtelomeric regions. This histone modification is controlled by the histone deacetylase PfSir2—however, only for a subset of variant gene family members—revealing an unusual mechanism of PfSir2 repression distinct from the postulated telomere position effect. In addition, this study allowed us to identify subtelomeric gene families not yet characterized, which are apparently differentially transcribed and represent potential virulence factors participating in phenotypic plasticity of malaria parasites.

RESULTS

H3K9me3 Shows a Highly Localized Atypical Distribution in *P. falciparum* Chromosomes

We performed ChIP-chip analysis to determine the localization of H3K9me3 across the *P. falciparum* 14 chromosomes. Because most of the dynamic histone modification changes controlling gene regulation in *P. falciparum* appear to occur in the flanking noncoding regions (Cui et al., 2007; Lopez-Rubio et al., 2007) and to take advantage of the small size of the parasite genome, we developed a custom-made high-resolution tiling array covering coding, intergenic, and also noncoding subtelomeric regions (for details, see Supplemental Experimental Procedures available online). We observed several prominent H3K9me3-enriched domains restricted to all subtelomeric regions as well as to internal regions of chromosomes 4, 6, 7, 8, and 12 (Figure 1A). ChIP-chip analysis of another repressive mark (H4K20me3) and activation marks (H3K4me3 and H3K9ac) showed a broad distribution across the genome (as exemplified for chromosome 12 in Figure 2), contrasting with the pattern of H3K9me3. H3K4me3 and H3K9ac were basically absent at the major heterochromatin loci coated with H3K9me3. Our results demonstrate the almost universal utilization of H4K20me3, H3K4me3, and H3K9ac, whereas H3K9me3 is highly restricted to chromosome ends and some internal regions.

P. falciparum chromosome ends display a conserved higher-order structure being composed of telomeric DNA followed by six repetitive noncoding polymorphic DNA blocks (TAREs 1–6), with an average total length of ~30 kb (Figueiredo et al., 2000). Because these regions are composed of repetitive DNA, our custom tiling array included probes only to the extremities of one chromosome (chromosome 12) (see Supplemental Experimental Procedures). We observed a strong enrichment in H3K9me3 in the entire TAREs 1–6 (Figures 1B, right, 2, both flanks, and S1). On the contrary, telomeric repeat DNA presented only a modest H3K9me3 level (Figure S1, right). H3K4me3 and H3K9ac were completely absent from TAREs and telomere repeats, and H4K20me3 was detectable only at low levels (Figure 2, both flanks).

Eukaryotic centromeres and pericentromeric regions are embedded in heterochromatin and exhibit unique chromatin architecture necessary for their chromosome segregation function (Grewal and Jia, 2007). *P. falciparum* centromeric DNA differs from centromeres of other organisms. It consists of AT-rich (97%) domains with a sharply defined size limit of 2.3–2.5 kb, which lack interchromosomal conserved motifs (Kelly et al., 2006). Our tiled array also covered pericentromeric DNA. In contrast to other organisms in which this region is enriched in H3K9me3, our ChIP-chip analysis showed that pericentromeric chromatin in *P. falciparum* was not enriched for H3K9me3 (example for pericentromere in Figure 2), which is consistent with the unusual nature of centromeric DNA in this parasite.

H3K9me3 Is Associated with Differentially Transcribed Virulence Gene Families

Detailed examination of the major heterochromatin regions revealed that the entire *var* gene family was enriched in H3K9me3, which agrees with previous predictions (Chookajorn et al., 2007; Lopez-Rubio et al., 2007). In addition, we observed that many distinct gene families adjacent to subtelomeric *var* genes were also enriched in H3K9me3 in the 5′UTR and coding region (Figure 1B). Chromosome internal H3K9me3-enriched domains contained generally only *var*, *rif*, and *stevor* genes (Figure 1C). We found H3K9me3 enrichments in seven previously identified subtelomeric gene families: *var*, *rif*, *stevor*, *Pfmc-2TM*, *clag*, *PfAcs*, and *PHIST* (Table 1). For almost all of these gene families, there are experimental evidences demonstrating a differential transcription mode of individual members. Another common feature is that many of these gene families code for variant surface proteins participating in the vast phenotypic plasticity of blood stage parasites and immune evasion (Scherf et al., 2008a).

Additionally, based on our H3K9me3 findings together with OrthoMCL database (Chen et al., 2006), we identified five putative subtelomeric gene families. In the absence of any biological data, we called these families PFD0075w-like, PF14_0742-like, PF14_0758-like, PF14_0743-like, and MAL8P1.335-like (Table 1). Published expression profile data of these genes (Le Roch et al., 2003) analyzed using PlasmoDB (http://plasmodb.org/plasmo/) strongly suggest a differential transcription profile of these gene families, which is a hallmark for phenotypic variation. Silent members presented high levels of H3K9me3, whereas transcribed members had low levels of this mark in the 5′UTR (Table 1). Therefore, our results indicate that H3K9me3 in the 5′UTR may predict genes that are controlled by a similar epigenetic mechanism.

However, our analysis also showed that some subtelomeric gene families were not enriched for H3K9me3, such as *surfin*,

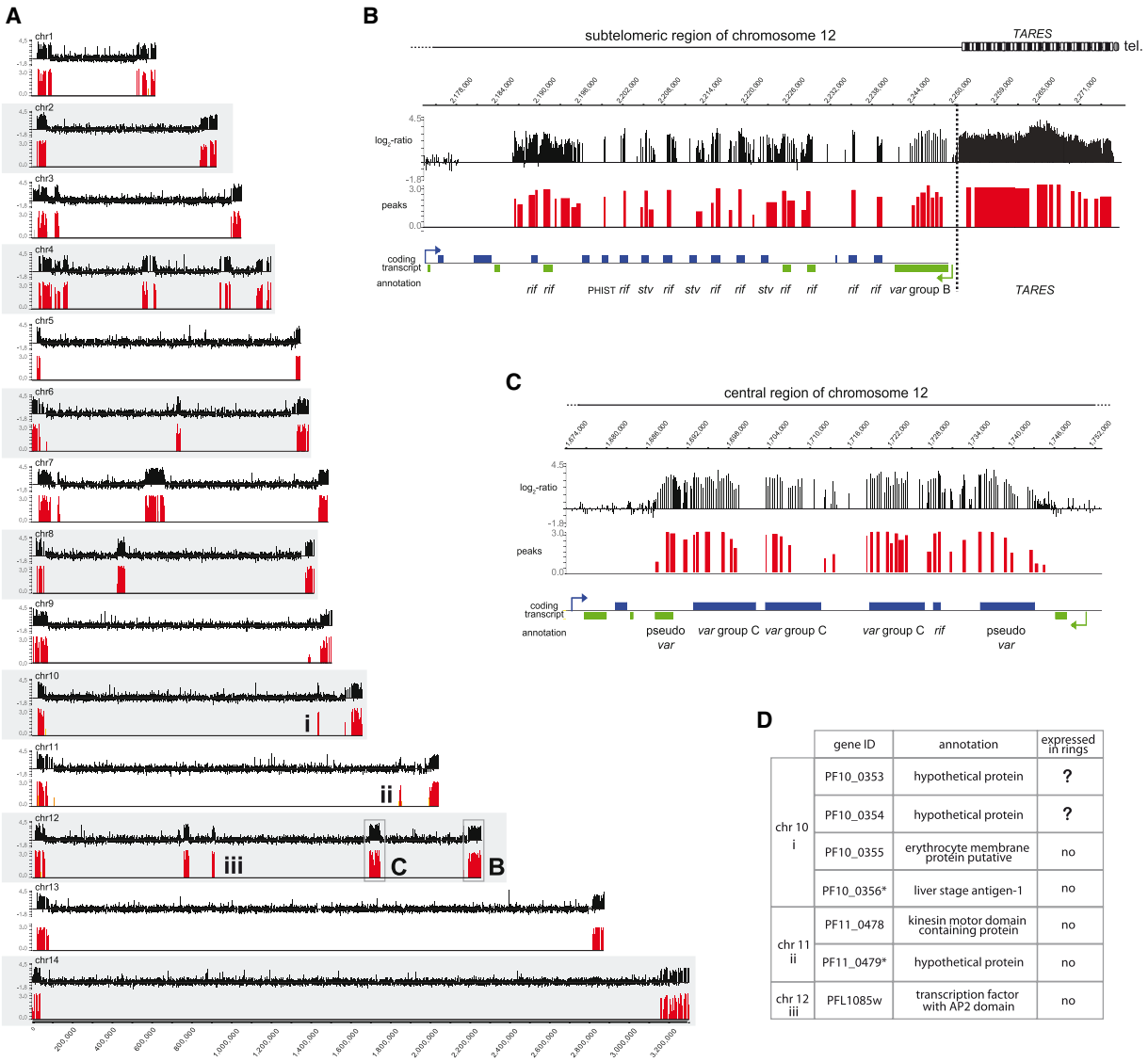

D

	gene ID	annotation	expressed in rings
chr 10 i	PF10_0353	hypothetical protein	?
	PF10_0354	hypothetical protein	?
	PF10_0355	erythrocyte membrane protein putative	no
	PF10_0356*	liver stage antigen-1	no
chr 11 ii	PF11_0478	kinesin motor domain containing protein	no
	PF11_0479*	hypothetical protein	no
chr 12 iii	PFL1085w	transcription factor with AP2 domain	no

Figure 1. ChIP-chip Genome Map of H3K9me3

(A) Paired tracings of raw data (top tracing for each chromosome) and the distribution of peaks (lower tracing for each chromosome) of H3K9me3 in the *P. falciparum* 14 chromosomes (noncoding chromosome ends are excluded). Regions represented in (B) and (C) are boxed. Regions analyzed in (D) are marked with i, ii, and iii.

(B) H3K9me3 distribution at telomeric and subtelomeric regions of chromosome 12. TAREs and coding regions are separated with a dotted line.

(C) H3K9me3 distribution for an internal H3K9me3-enriched domain in chromosome 12. Paired tracing for (B) and (C) as in (A).

(D) Table presenting H3K9me3-enriched genes that are neither *var* genes nor genes associated with *var* gene loci. Transcriptional data were collected from PlasmoDB. Gene marked with asterisk indicates that the enrichment covers partially the locus.

In all cases, raw data are presented as the log2 ratio of the hybridization signal given by DNA immunoprecipitated using specific antibody against H3K9me3 compared with the signal given by the input DNA sample. Peak data are represented as described in the Supplemental Experimental Procedures. The position on the genome sequence is indicated at the bottom for (A) and at the top for (B) and (C). The position and annotation of the predicted genes are presented at the bottom (coding DNA sequence; blue bars, sense; green bars, antisense).

FIKK, and *ETRAMP* (Table S1). These genes were interspersed into H3K9me3-enriched regions, resulting in a mosaic pattern of this histone modification. The question arises of whether these non-H3K9m3-enriched gene families are differentially transcribed or not. For the 20 member *FIKK* family, quantitative PCR data show that some members are transcribed at low levels during blood stage development (Nunes et al., 2007). For the *surfin* and *ETRAMP* families, expression profile data (PlasmoDB) show that some members are not expressed during blood stages. Further quantitative expression data of cloned parasites are necessary to determine whether these families undergo clonal variation.

We also detected three H3K9me3 short-ranged peaks outside of the large *var*-defined heterochromatic domains on chromosomes 10, 11, and 12 (Figure 1A, i, ii, and iii, respectively). Genes encoded in these heterochromatic ''islands'' are listed in

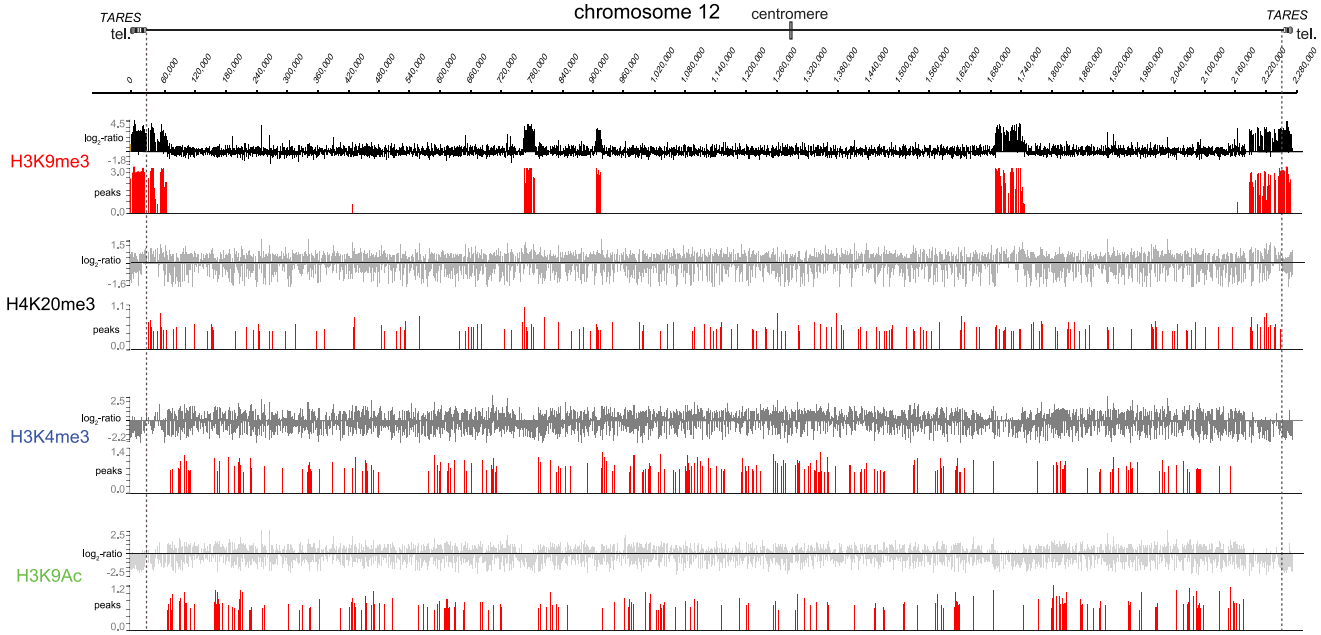

Figure 2. Chromosome 12 Distribution Profiles of Different Histone Modifications

The raw data (top tracing) and the distribution of peaks (lower tracing) identified for H3K9me3, H4K20me3, H3K4me3, and H3K9ac are presented. Noncoding chromosome ends (TAREs and telomeres) are separated with a dotted line. A schematic representation of chromosome 12 showing main features and the position on the genome is indicated at the top. Raw and peak data are presented as in Figure 1.

Figure 1D. Apart from PFL1085w, which encodes a member of the ApiAP2 family of transcription factors (De Silva et al., 2008), very little information is available for the other genes. Further analysis is needed to determine whether these genes participate in phenotypic diversity of parasites or are epigenetically coregulated.

PfKMT1 and H3K9me3-Enriched Genes Are Localized to the Nuclear Periphery

Given the unusual highly localized H3K9me3 pattern in *P. falciparum* genome, we were interested in investigating the nuclear organization of H3K9me3 domains. H3K9 methylation is performed by a histone lysine 9 methyltransferase KMT1 (Allis et al., 2007), of which an homolog (PF08_0012) has been found in *P. falciparum* genome (Cui et al., 2008). Antibodies raised against the *P. falciparum* KMT1 were used to study the cellular location of this molecule. Surprisingly, we observed that PfKMT1 fluorescent signals located largely at the periphery of *P. falciparum* nuclei (Figure 3A). Likewise, antibodies specific for H3K9me3 showed a predominant enrichment in the perinuclear space (Figure 3A), strongly suggesting that H3K9me3-enriched genes might locate in this nuclear compartment.

To test this hypothesis, we performed a quantitative large-scale localization study of genes enriched in H3K9me3 using fluorescent in situ hybridization (FISH). We chose to examine the entire *var* gene family and two non-*var* genes, which form distinct H3K9me3 peaks at internal (PFL1085w) and subtelomeric chromosomal positions (PF11_0479) (Figures 1A and 1D, iii and ii, respectively). For analysis of the *var* 60 members, we used exon2 probes that crosshybridize to *var* genes of each major group: group A (10 subtelomeric genes), group B (22 subtelomeric genes), and group C (13 genes grouped in 7 internal regions) (Lavstsen et al., 2003) (Figures 1A and 3B). We observed two to five foci per nucleus for each *var* exon2 probe, indicating clustering of *var* genes from groups A, B, and C (Figures 3C and S2). The other FISH probes tested were gene-specific probes (single internal *var* PFF0845c, PF11_0479, and PFL1085w) and produced single foci per nucleus (Figure 3C).

In order to precisely define the nuclear boundaries, we developed an antibody that recognizes a *P. falciparum* protein encoded by a gene orthologous to a yeast nuclear pore protein (PF14_0706) (Figure S3). The area of the nuclear section obtained in immunofluorescence staining was calculated and then divided into equal thirds. FISH signals were scored as localizing to zones 1, 2, and 3 (Hediger et al., 2002), as illustrated in Figures 3C and S3. Quantitative analysis of nuclear position revealed that all *var* and non-*var* genes enriched for H3K9me3 and analyzed were not randomly distributed but, rather, located predominantly at the nuclear periphery. By contrast, internal genes nonenriched in H3K9me3 were found mostly in internal nuclear regions (Figures 3C and S4). Thus, virulence gene families and single-copy genes enriched in H3K9me3 are localized at the perinuclear space, irrespective of their chromosomal position. This led us to hypothesize that PfKMT1 and H3K9me3 might determine the nuclear organization of genes.

P. falciparum chromosome ends are tethered to the nuclear membrane forming clusters (Freitas-Junior et al., 2000). To exclude the possibility of internal H3K9me3-enriched genes (*var* group C, *var* PFF0845c, and PFL1085w) being at the nuclear periphery as a consequence of being associated to telomeric clusters, we analyzed their relative position to these clusters. Simultaneous FISH analysis of *var* exon2C with a telomeric

Table1. Subtelomeric Gene Families Enriched in H3K9me3

Name	Number of Members	Expressed Members/Total Number of Members	H3K9me3 Enriched at: Silenced Member	Active Member[a]	Comments
PfEMP1/var	60	1/60	yes	no	cytoadherence immune escape immunomodulation IE surface
RIFIN	150	several/130	yes	no data	IE surface PVM
STEVOR	39	1/39[b]	yes	no data	IE surface PVM
PfMC-2TM	13	1/13[b]	yes	no data	IE surface PVM
PfACS	10	~6/10	yes	no	metabolic protein
clag					
clag3.1/clag3.2	2	1/2	yes	no	invasion rhoptry protein
clag2/clag8/clag9	3	3/3	-	no	
PHIST					
PHISTa	23	~6/23	yes	no	pexel
PHISTb	25	20/25	yes	no	pexel
PHISTb (RESA)	7	6/7	yes	no	pexel
PHISTc	16	most of them	no	no	pexel
[e]PFD0075w-like	10	1/10	yes	no	TM
[e]PF14_0742-like	5	1/5	yes	no	TM
[e]PF14_0758-like	3	1/3	yes	no	TM
[e]PF14_0743-like	4	2/4	yes	no	TM
[e]MAL8P1.335-like	4	~1/4[c]	yes[d]	no data	

IE, infected erythrocyte. PVM, parasitophorus vacuole membrane. TM, transmembrane domain.
[a] At least in the 5′ flanking regions.
[b] Clonally variant family in which one dominant member is expressed, although some clones do not express any.
[c] Only data for two members.
[d] Microarray covers only 3′ regions of some members.
[e] OrthoMCL DB recognizes several paralogs.

cluster marker TARE6 demonstrated that *var* group C clusters localized randomly relative to chromosome end clusters (Figure 3D). Similar random distribution was obtained for colocalization of TARE6 with 5′UTR from *var* group C and the single internal *var* PFF0845c (data not shown), thus suggesting that perinuclear tethering of chromosome internal genes is independent of telomeric clustering. Taken together, our results indicate that heterochromatic peripheral region is composed of telomeric and nontelomeric clusters. Moreover, it implies that certain *Plasmodium* chromosomes (the case of chromosome 12, which has several domains of H3K9me3 enrichment; see mapping of nuclear position of different loci in Figure S4) should form several large loops into the nuclear membrane, as exemplified in Figure 3F.

RNA FISH Locates *var* Transcripts to the Nuclear Periphery Dissociated from Telomeric Clusters

Previous work has demonstrated that, upon activation of a *var* gene (*var2CSA*), H3K9me3 in the 5′UTR is lost but persists in the 3′coding region (Lopez-Rubio et al., 2007). It has also been shown that the active *var2CSA* gene locates at the nuclear periphery. However, there are conflicting conclusions with regard to its association with the telomeric clusters (Scherf et al., 2008b). To overcome potential problems linked to DNA FISH, such as possible relocation of the *var2CSA* gene to telomeres once transcription ceases, we located *var2CSA* transcripts using RNA FISH. Telomeric clusters were then visualized performing a second hybridization using the TARE6 probe by DNA FISH. We observed that *var2CSA* transcripts were clearly dissociated from telomeric clusters (Figure 3E).

To rule out the possibility that this observation was specific for the *var2CSA* gene, we localized transcripts of the entire *var* gene repertoire. We performed RNA/DNA FISH using the exon2 *var* group-specific probes. We observed that mRNA transcripts from the different *var* groups did not associate with the telomeric clusters (Figure 3E), implying that activation of any *var* gene involves nuclear reposition into a peripheral region compatible with transcription. With regard to *var* group A and B, which are physically linked to telomeric repeats, activation involving acquisition of active chromatin marks, such as H3K9ac and H3K4me2/3, presumably leads to chromatin decondensation and formation of a single-gene loop, which separate out the transcribed gene from more compact and silent telomeric clusters (schematically shown in Figure 3F). Although anchoring at the nuclear periphery must require appropriate proteins, the fact that the H3K9me3 subsists in the active gene (in the 3′ coding region) may be important for maintenance of the gene in a perinuclear position.

PfSir2 Controls H3K9me3 in a Discontinuous Manner

In order to determine whether the putative PfKMT1 was responsible for H3K9 methylation and its role in the localization of heterochromatin domains to the nuclear periphery, we

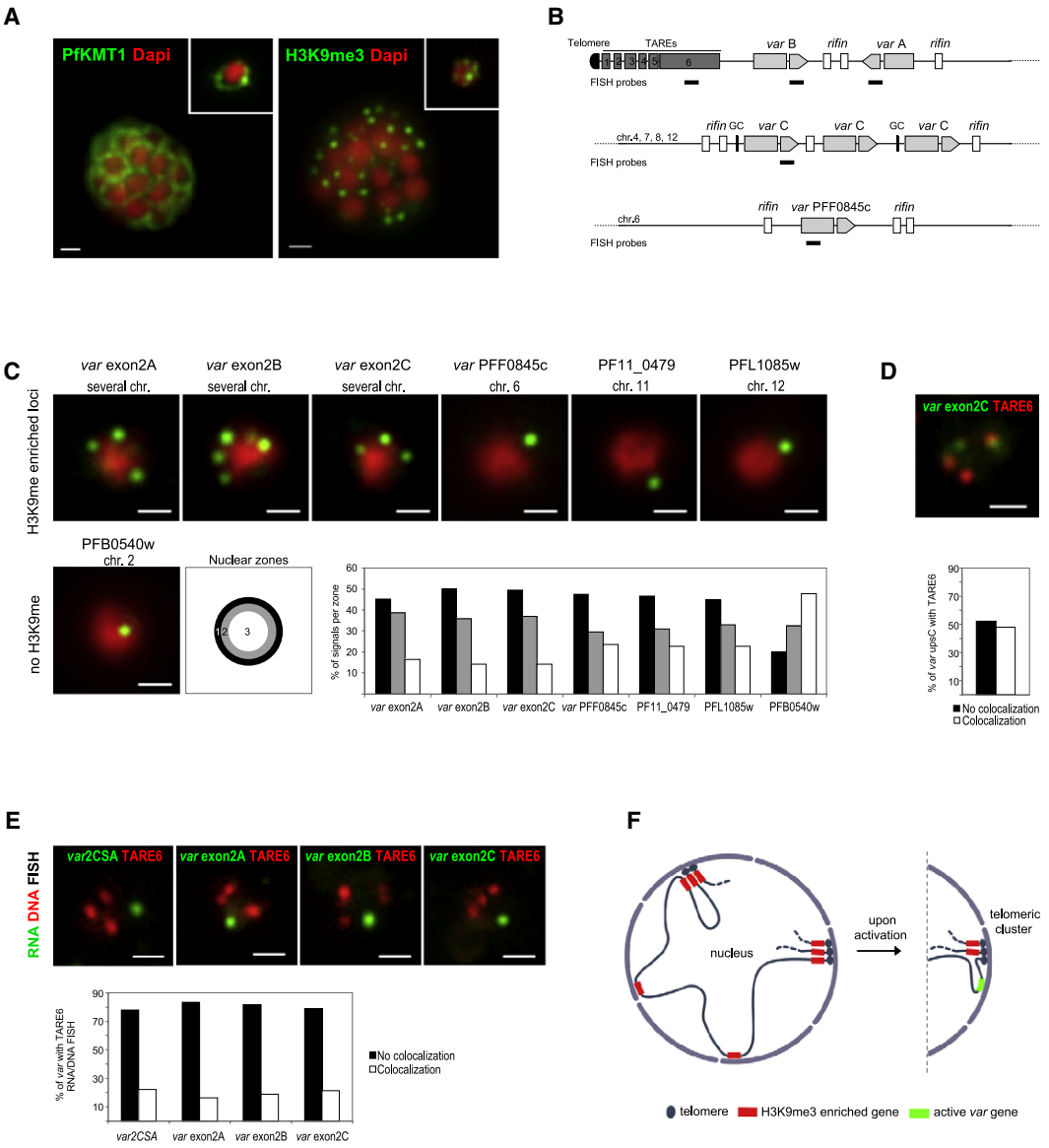

Figure 3. PfKMT1 and Genes Enriched in H3K9me3 Are Positioned at the Nuclear Periphery

(A) Immunofluorescence assays using antibodies against H3K9me3 (right) and the *P. falciparum* putative H3K9 methyltransferase PfKMT1 (left). 3D7 parasites are in late schizont (main image) and ring stage (top-right square). Nuclear DNA was detected with Dapi (red).

(B) Schematic of the *var* loci organization. Each *var* gene consists of a large variable exon1 (4–9 kb) and a conserved exon2 (~1.5 kb). The 60 member *var* gene family can be divided into three major groups (A, B, and C) based on chromosome location and sequence similarity. Group A contains 10 telomeric genes transcribed toward the telomere; 22 telomeric genes belong to group B and are transcribed toward the centromere; and group C includes 13 internal genes (Lavstsen et al., 2003). Among the *var* arrays, there are members of other multigene families, such as *rifin* and *stevor*. The location of FISH probes is indicated with horizontal bars.

(C) DNA FISH analysis of 3D7 ring stage parasites nuclei. (First row) Subtelomeric (*var* exon2A, *var* exon2B, and PF11_0479) and internal H3K9me3-enriched genes (*var* exon2C, *var* PFF0845c, and PFL1085w). (Second row) Internal gene nonenriched in H3K9me3 (PFB0540w). FISH signals are in green, and the nuclear DNA was stained with Dapi (red). (Bar graph) Subnuclear position of FISH signals with respect to three concentric zones of equal surface (zones 1, 2, and 3). The number of nuclei analyzed and the 95% confidence values (p) for the χ^2 test between random and test distributions are: *var* exon2A n = 143, p = 1.50×10^{-8}; *var* exon2B n = 166, p = 3.02×10^{-16}; *var* exon2C n = 194, p = 6.92×10^{-15}; *var* PFF0845c n = 180, p = 1.90×10^{-2}; PF11_0479 n = 226, p = 7.59×10^{-3}; PFL1085w n = 159, p = 5.30×10^{-2}; PFB0540w n = 151, p = 1.10×10^{-2}.

(D) Two-color DNA FISH of *var* exon2C probe (green) and telomeric clusters (TARE6 probe) (red) on 3D7 ring stage parasites. Nuclear DNA was detected with Dapi (data not shown). (Bar graph) Colocalization was 48.06% (n = 105), and the 95% confidence value (p) for the χ^2 test between random and test distributions was p = 0.615.

(E) RNA/DNA FISH analysis of *var* transcripts and telomeric clusters. (First row) RNA FISH signals are shown in green, and DNA FISH signals are shown in red (TARE6 probe). Nuclear DNA was visualized with Dapi (data not shown). *var2CSA* transcripts were detected in ring stage FCR3-CSA-selected parasites (first image). Exon2 probes of each *var* group were hybridized on bulk-cultured 3D7 ring stage parasites. (Second row) Quantification of colocalization of *var* transcripts with telomeric clusters (*var2CSA* 77.94% of noncolocalization, n = 68; *var* exon2A 83.64%, n = 55; *var* exon2B 81.48%, n = 54; *var* exon2C 78.95%, n = 38).

attempted to disrupt the unique *PfKMT1* locus. Using the currently available knockout methods for *P. falciparum*, we were incapable of generating viable parasites without *PfKMT1*. H3K9 trimethylation requires the action of a histone deacetylase to remove the acetyl group before the methylation step (Nakayama et al., 2001). We used a parasite knockout strain for the histone deacetylase PfSir2 (Duraisingh et al., 2005) to analyze the molecular events leading to derepression of a subset of subtelomeric genes and its role in the formation of heterochromatin and nuclear organization. ChIP-chip analysis of *PfSir2*-disrupted 3D7 parasites showed that H3K9me3 levels were reduced and H3K9ac levels were increased, compared to wild-type parasites, in the 5′UTR of the previously published upregulated genes (Figure 4 and Table 2). Competition between acetylation and methylation at H3K9 in the 5′UTR has been previously shown to influence transcription activity of *var* genes (Lopez-Rubio et al., 2007). In the absence of PfSir2, apparently this balance is disturbed in favor of H3K9ac. Unexpectedly, this effect is seen only in 2 out of 12 gene families enriched in H3K9me3, the *var* and *rif* (Figures 4A–4D). Our results suggest that PfSir2-mediated H3K9 deacetylation is required for establishing repressive H3K9 methylation for a subset of *var* and *rif* genes.

Surprisingly, the lack of PfSir2 resulted in very local effects in a discontinuous manner (Figures 4A–4D). The postulated telomere position effect of PfSir2 (Freitas-Junior et al., 2005) would have predicted a continuous H3K9me3 depletion from the telomere into the coding region. Together, these data suggest that different separated DNA regions may interact with PfSir2 via small loop formation (schematically shown in Figure 4G). Consistent with this confined effect of PfSir2 in H3K9me3, analysis of the nuclear localization of PfKMT1 and H3K9me3-enriched genes in Δ*PfSir2* parasites did not produce major changes (data not shown).

A number of additional puzzling features of PfSir2 emerged from our study. First, a general decrease of H3K9me3 with no increase of H3K9ac in basically all intergenic regions of the heterochromatic domains was observed, even in genes whose transcriptional state did not change (Figure 4E). Second, nearly the entire subtelomeric domain in the left arm of chromosome 7 (comprising 13 members of gene families) was depleted of H3K9me3, and H3K9ac levels remained low (Figure 4F). Unfortunately, there are no available transcription data for these loci in *PfSir2*-disrupted parasites to see whether the absence of H3K9 methylation without induction of acetylation affects repression. Third, we observed only a weak reduction of H3K9me3 at subtelomeric repeats (Figure S1) associated to a slight increase in H3K9ac, suggesting that other histone deacetylases may cooperate with the process of H3K9me.

DISCUSSION

In this study, we demonstrate a link between malaria parasite virulence genes enriched for H3K9me3, their spatial location at the nuclear periphery, and their epigenetic silencing via a perinuclear repressive center. This unique association is almost entirely restricted to clonally variant multigene families involved in phenotypic plasticity.

Here, we established a high-resolution genome-wide H3K9me3 heterochromatin map for a malaria parasite. *P. falciparum* chromosome end regions (TAREs 1–6) are enriched in H3K9me3 and may represent constitutive heterochromatin, like in other organisms. The formation of heterochromatin in association with repetitive sequences is apparently crucial for functional organization of chromosome ends (Grewal and Jia, 2007). In contrast to other organisms, however, no enrichment was found on pericentromeric DNA, and high enrichment was found in all subtelomeric coding regions. A few small blocks of H3K9m3 were also detected in chromosome internal regions (Figure 1). Other histone modifications showed a broad distribution along chromosomes (Figure 2), and their genome-wide link to gene expression has been initiated in collaboration with PlasmoDB. The fact that we used a high-resolution tiling array including noncoding regions may explain why, in a previous ChIP-chip study using only coding regions with a very low coverage, the authors did not observe the restricted localization of H3K9me3 (Cui et al., 2007).

Importantly, we found five subtelomeric gene families not yet characterized, which are enriched in H3K9me3, differentially transcribed, and that may participate in the phenotypic makeup of genetically clonal blood stage parasites. Insight into these potential virulence factors is very important for our understanding of malaria pathogenesis. It is noteworthy that other variant gene families such as *surfin*, *FIKK*, and *ETRAMP* (Table S1), which are not enriched in H3K9me3, are interspersed within the subtelomeric region, demonstrating that two types of gene families, apparently controlled by distinct mechanisms, coexist in *P. falciparum* subtelomeres.

The data also reveal that epigenetic boundaries do exist in the heterochromatin domains to prevent the spreading of the repressive mark into neighboring regions. We provide genome-wide, precise physical limitations for H3K9me3 in *P. falciparum*. It has been suggested that RNA polymerase III (Pol III)-transcribed genes act as barriers against self-propagating heterochromatin in single-celled eukaryotes (Lunyak, 2008). Indeed, some tRNA genes localize in the proximity of heterochromatin domain borders of *P. falciparum* (for example, in chromosome 4 left end and chromosome 13 right end). Assays need to be developed to elucidate whether Pol III-transcribed genes or other specific DNA elements are involved in blocking the spreading of H3K9me3.

The present work highlights the idea that *P. falciparum* genomic DNA is nonrandomly distributed in the nucleus and that gene expression and spatial organization are strongly linked (see the model in Figure 3F). Nuclear position analysis of actively transcribed *var* genes, in their native chromosomal context, confirmed their dissociation from telomeric clusters. We speculate that chromatin loop formation may be associated with activation and relocation of subtelomeric *var* genes in a

In all cases, representative examples are shown as merged images, FISH signals were scored using nuclei from multiple experiments, and scale bars represent 1 μm. For quantification of colocalization, only nuclei containing at least three TARE6 signals were considered as positive, and colocalization was defined as any overlap between two fluorescent signals.
(F) Proposed model for nuclear organization of H3K9me3-enriched domains. The chromosome 12 was used as an example (see text for details).

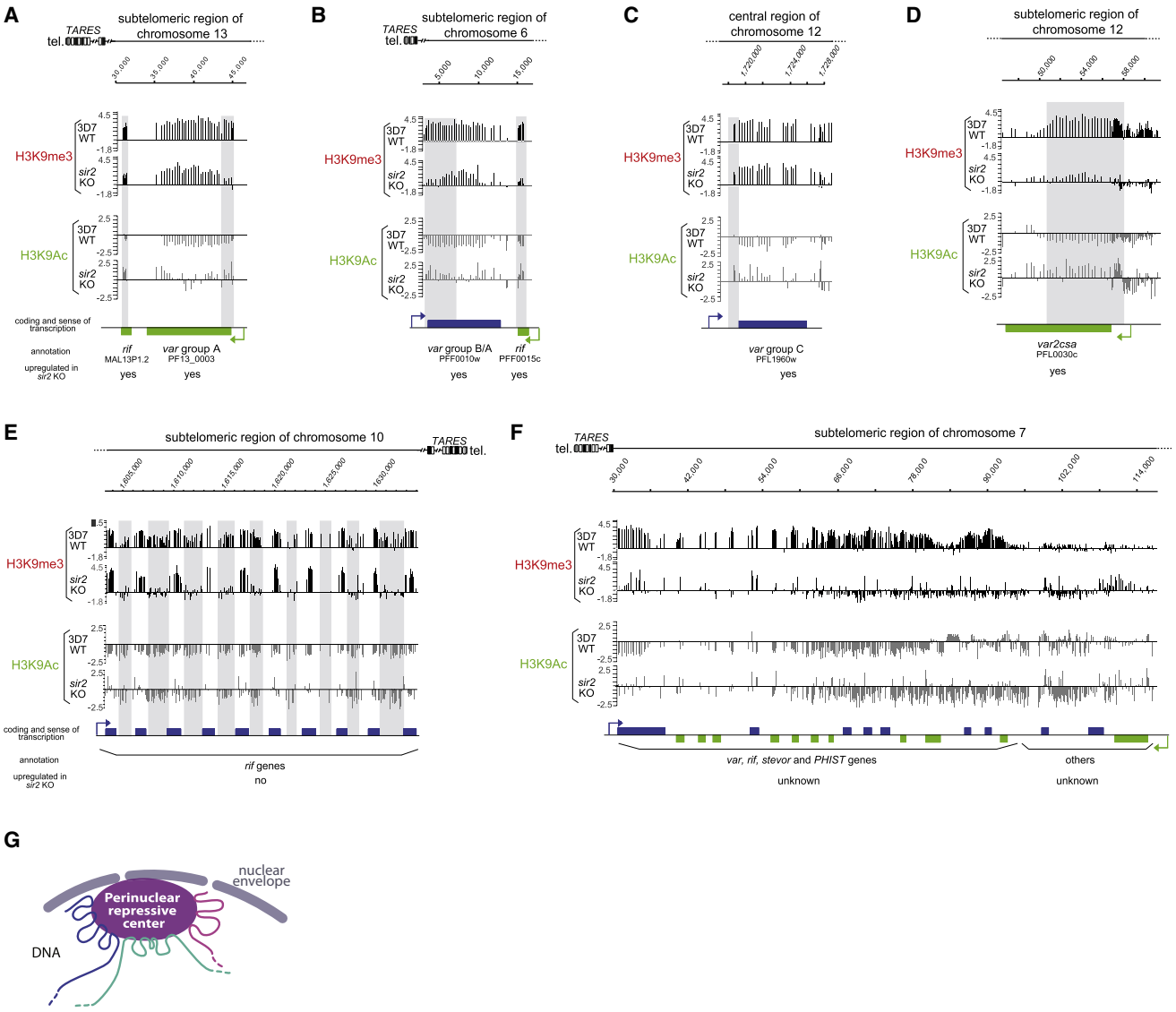

Figure 4. ChIP-chip Analysis of PfSir2 Knockout Parasites

Raw data for H3K9me3 (black) and H3K9ac (gray) in 3D7 wild-type (WT) and *sir2* KO parasites. Schematic representation of the analyzed regions showing main features and the position on the genome is indicated at the top. The position, annotation, and whether upregulated or not in *sir2* KO parasites of the predicted genes are presented at the bottom.

(A–D) Local effects: decrease of H3K9me3 and increase of H3K9ac in the 5′UTR of *var* and *rif* genes.

(E and F) Regional effects: decrease of H3K9me. Gray squares highlight the regions with histone modification changes. Transcription data have been obtained from PlasmoDB. Raw data are presented as in Figure 1.

(G) Proposed model for a common epigenetic default silencing mechanism at the nuclear periphery for gene families linked to virulence. Intergenic DNA regions may interact with perinuclear repressive centers (PERC) via small loop formation. We hypothesize that PERC is composed of PfSir2, PfOrc1, PfHP1, PfKMT1, and presumably other histone deacetylases.

subperinuclear transcriptional-competent region that might be specific for *var* genes (Ralph et al., 2005). The expression of two distinct *var* promoters in a similar perinuclear location provides additional evidence for a *var*-specific expression site (Dzikowski et al., 2007). Relocalization of a subtelomeric gene from a telomeric focus associated with transcriptional activation has also been described in *S. cereviseae* (Taddei et al., 2006). Notably, induction of the same gene through an alternative artificial pathway produces relocalization to a different region in the yeast nucleus. This underlines the importance of the natural chromosomal context to decipher epigenetic mechanisms of gene activation.

One of the most striking findings is that perinuclear large loop formation of internal chromosome coding regions is associated with H3K9me3 (Figures 3 and S4), and this is independent of either telomeric clustering or a GC-rich element. This ~200 bp GC-rich element apparently produces noncoding RNAs and is strictly associated with internal *var* arrays, although it is not found

Table 2. Histone Changes Linked to Derepressed *var* Genes in Δ*PfSir2* Parasites

var Group	PlasmoDB Accession Number	H3K9me3 Levels in the 5′ Flanking Region in Δ*PfSir2* Parasites	H3K9ac Levels in the 5′ Flanking Region in Δ*PfSir2* Parasites	Fold Expression ΔPfsir2/WT[a]	
				Experiment 1	Experiment 2
var2CSA	PFL0030c	low	high	2	10
group A	PF13_0003	low	high	100	90
group A	PFA0015c	low	high	50	30
group A	PFF0020c	low	low	19	3
group A	PFD1235w	no data	no data	11	7
group B/A	PFF1580c	low	high	24	22
group B/A	PFF0010w	low	high	36	29
group B/C	PF07_0050	low	high	67	34
group C	PFL1960w	low	high	26	12

[a] (Duraisingh et al., 2005). Only genes with fold expression Δ*PfSir2*/WT ≥ 10 are shown.

near the single internal *var* genes on chromosomes 6 and 12 (Hall et al., 2002; Mourier et al., 2008). Together, our observations point to PfKMT1 and H3K9me3 as determinants of spatial organization of chromosomes in *P. falciparum* nuclei. This is supported by data obtained in *S. pombe* showing SpKMT1 to be crucial for correct subnuclear localization of the mating type region (Alfredsson-Timmins et al., 2007). In *P. falciparum*, however, deletion of PfKMT1 produces a lethal effect on parasite proliferation. Improved inducible gene knockdown systems will be necessary to gain insight into the PfKMT1 function in spatial organization of *P. falciparum* nuclei.

Our results are compatible with the existence of ''perinuclear-repressive centers'' (PERC) (see model in Figure 4G) composed of PfSir2 and other potential silencing factors such as PfOrc1 (Mancio-Silva et al., 2008), PfHP1 (A.S. and R. Hernandez-Rivas, unpublished data), and probably PfKMT1. Although experiments are needed to clarify whether these telomeric-associated proteins form complexes, evidences from studies in *S. pombe* (Bannister et al., 2001; Nakayama et al., 2001; Yamada et al., 2005) indicate that H3K9me provides the binding site for HP1 to recruit other proteins, such as histone deacetylases and methylases, involved in heterochromatin stabilization and spreading. DNA-binding proteins and/or transcribed repetitive subtelomeric noncoding RNAs (Mourier et al., 2008) are possibly involved in the initial targeting of histone-modifying enzymes to the PERC. It will be also interesting to investigate whether telomeric and internal heterochromatic regions share the same PERC components.

Having established high-resolution ChIP-chip assays for *P. falciparum*, we were in a position to analyze chromatin changes in PfSir2 mutant parasites, which display transcriptional derepression of a subset of *var* and *rif* genes (Duraisingh et al., 2005). We show that PfSir2 acts precisely on H3K9 methylation in the 5′UTR of genes, which have been shown to be upregulated in Δ*Pfsir2* parasites. The discontinuous pattern of H3K9me3 removal along subtelomeric regions and replacement by acetylation was unexpected given the current model of telomere position effect, which predicts a gradient along the telomere into the subtelomeric coding regions (Freitas-Junior et al., 2005; Mancio-Silva et al., 2008). The results strongly suggest a distinct mechanism of PfSir2-mediated silencing. We hypothesize that multiple small loop structures of chromosome regions harboring variant multigene families interact directly with PERC (see model in Figure 4G). In the case of PfSir2, this interaction appears to focus in the 5′UTR of some *var* and *rif* genes, underlining the important role of this DNA region in *var* gene control.

Several elements suggest that subtelomeric chromatin is made up of other histone deacetylases. First, PfSir2 only controls repression of a small subset of the H3K9me3-enriched genes (5%), and second, PfSir2 inactivation has no major change in the H3K9me3 levels in the noncoding subtelomeric region. This is in contrast to *S. pombe*, wherein loss of Sir2 resulted in a general decrease in H3K9me3 and an increase in H3K9ac at telomeres and telomeric-associated sequences (Shankaranarayana et al., 2003). We had searched in the *P. falciparum* genome for other Sir-like genes and found an open reading frame on chromosome 14 that is homologous to human Sirt6, which acts at subtelomeric repeats (Michishita et al., 2008). Antibodies raised against this protein show a similar location at the nuclear periphery as PfSir2 (L.M.-S. and A.S., unpublished data), strongly suggesting that a second telomere-associated histone deacetylase contributes to epigenetic silencing of virulence gene families.

In conclusion, our study demonstrates that *P. falciparum* has a specific mechanism to restrict repressive H3K9me3 almost exclusively to clonally variant gene families. Moreover, our data show a complex spatial distribution of plasmodial chromosomes in the nucleus, which apparently creates functional distinct compartments that are important for epigenetic gene expression of a subgroup of genes. We postulate that distinct DNA loops may exist: large chromosomal loops, which bring specific chromosome regions to the nuclear periphery; small DNA loops that allow interaction with different components of PERC; and chromatin loops associated with relocation from telomeric clusters of active genes into a perinuclear expression site. In addition, we provide a detailed insight into the underlying chromatin modifications that are necessary to overcome the precise monoallelic counting mechanism of *var* genes. Our PfSir2 mutant analysis demonstrates that the removal of the H3K9me3 and replacement by acetylation in the 5′UTR is a key step toward unlocking the default silent state of *var* genes. It will be interesting to investigate whether other protozoan pathogens that rely on subtelomeric gene families for immune escape (Borst, 2003) may use this type of epigenetic silencing mechanism. Insight into the complexity of control of gene families involved in malaria

pathogenesis is vital for understanding the disease and will provide a major step toward controlling it.

EXPERIMENTAL PROCEDURES

Parasites

P. falciparum blood stage parasites were cultivated in the conditions previously described (Nunes et al., 2007). The 3D7Δ*Sir2* parasites were cultivated in the presence of 2 μM Pyrimethamine. Selection of FCR3 parasites for CSA binding was performed according to Scherf et al. (1998).

Antibodies

Antibodies against histone modifications were purchased from Upstate for H3K9me3, H3K9ac, and H4K20me3 (07-442, 07-352, and 07-463, respectively) and from Abcam for H3K4me3 (ab8580). To obtain polyclonal antibody serum against PfKMT1, we used GenScript Corporation standard protocols for immunizing a rabbit with a synthetic peptide (N-CASRDIQPNEPLKYH-C).

Custom *P. falciparum* High-Resolution Tiling Array Design

The design of the array was done with the assistance of NimbleGen Systems Inc. We downloaded the *P. falciparum* genome sequence from The Sanger Center website and subjected it to several iterative rounds of probe selection (see Supplemental Experimental Procedures).

ChIP-chip Analysis

ChIP assays were carried out as previously described (Lopez-Rubio et al., 2007) using ring stage unselected 3D7 parasites.

We subjected precipitated DNA and DNA from parasite extracts (input) recovered after reverse crosslinking to amplification using Sigma GenomePlex WGA kit. After amplification, the immunoprecipitated DNA was tested for enrichment of control loci by qPCR (Realplex4 EpgradientS thermalcycler, Eppendorf). DNA was labeled, hybridized, and the data extracted according to standard operating procedures by NimbleGen Systems Inc. At least two biological replicates were performed for each condition and two technical replicates for each biological replicate. Detailed procedures and quantitative real-time PCR validation of ChIP-chip data are described in the Supplemental Experimental Procedures.

Immunofluorescence and FISH

Immunofluorescence assays were performed as previously described (Tonkin et al., 2004) for PfKMT1 and (Mancio-Silva et al., 2008) H3K9me3. Antibody dilutions were: anti-PfKMT1, 1:500; anti-H3K9me3, 1:500; and Alexa-Fluor-488-conjugated anti-rabbit highly crossabsorbed, 1:500.

For FISH, infected red blood cells were lysed with saponine and the released parasites fixed in suspension with 4% paraformaldehyde. Parasites were then deposited on microscope slides and subjected to DNA FISH in the conditions previously described (Mancio-Silva et al., 2008). For combined RNA/DNA FISH, parasites were deposited on slides, treated with 0.1% Triton X-100 for 5 min, and hybridized first with *var* probes at 50°C for 16 hr. The slides were washed three times in 2 × SSC at 50°C, denaturated at 80°C, and hybridized with the TARE6 probe at 37°C for 16 hr. Finally, the slides were washed as for DNA FISH.

TARE6 and *var2CSA* probes were obtained as described before (Ralph et al., 2005). All other FISH probes were PCR amplified from genomic DNA using the primers listed on Table S2. Images were taken using a Nikon Eclipse 80i microscope with a CoolSnap HQ2 camera (Photometrics). NIS Elements 3.0 software (Nikon) was used for acquisition and ImageJ (http://rsbweb.nih.gov/ij/) for composition. Chromatic aberration was corrected in all images by aligning the red, green, and blue channel signals from 0.2 μm TetraSpeck microspheres.

ACCESSION NUMBERS

Microarray data for ChIP-chip 3D7 and 3D7Δ*Sir2* parasites are available in the ArrayExpress database (www.ebi.ac.uk/arrayexpress) under accession numbers E-MEXP-1806 and E-MEXP-1805, respectively.

SUPPLEMENTAL DATA

The Supplemental Data include Supplemental Experimental Procedures, two tables, and four figures and can be found with this article online at http://www.cell.com/cell-host-microbe/supplemental/S1931-3128(09)00030-4.

ACKNOWLEDGMENTS

We would like to thank to A. Cowman for providing the 3D7Δ*Sir2* strain, M. Nunes for the FCR3-CSA selected parasites, D. Roos for help with annotation files for genome-wide analysis, E. Bischoff for assistance with microarray design, and PlasmoDB for the invaluable malaria database support. We are also grateful to B. Arcangioli, P. Navarro, and L. Riviere for critical reading of the manuscript and to A. Cordeiro da Silva and Faculdade de Farmácia (Universidade do Porto, Portugal) for their support. This work was financed by BioMAlPar (contract No: LSPH-CT-2004-503578). J.-J.L.-R. has financial support from the Human Frontier Science Program and L.M.-S. from the Portuguese Foundation for Science and Technology. A.S. is supported by a grant ANR Microbiologie (ANR-06-MIME-026-01) and Fonds Dédié (Sanofi-Avantis).

Received: September 23, 2008
Revised: December 5, 2008
Accepted: December 31, 2008
Published: February 18, 2009

REFERENCES

Alfredsson-Timmins, J., Henningson, F., and Bjerling, P. (2007). The Clr4 methyltransferase determines the subnuclear localization of the mating-type region in fission yeast. J. Cell Sci. *120*, 1935–1943.

Allis, C.D., Berger, S.L., Cote, J., Dent, S., Jenuwien, T., Kouzarides, T., Pillus, L., Reinberg, D., Shi, Y., Shiekhattar, R., et al. (2007). New nomenclature for chromatin-modifying enzymes. Cell *131*, 633–636.

Bannister, A.J., Zegerman, P., Partridge, J.F., Miska, E.A., Thomas, J.O., Allshire, R.C., and Kouzarides, T. (2001). Selective recognition of methylated lysine 9 on histone H3 by the HP1 chromo domain. Nature *410*, 120–124.

Barry, A.E., Leliwa-Sytek, A., Tavul, L., Imrie, H., Migot-Nabias, F., Brown, S.M., McVean, G.A., and Day, K.P. (2007). Population genomics of the immune evasion (var) genes of Plasmodium falciparum. PLoS Pathog. *3*, e34.

Blythe, J.E., Yam, X.Y., Kuss, C., Bozdech, Z., Holder, A.A., Marsh, K., Langhorne, J., and Preiser, P.R. (2008). Plasmodium falciparum STEVOR proteins are highly expressed in patient isolates and located in the surface membranes of infected red blood cells and the apical tips of merozoites. Infect. Immun. *76*, 3329–3336.

Borst, P. (2003). Mechanisms of antigenic variation: an overview. In Antigenic Variation, A. Craig and A. Scherf, eds. (London: Academic Press), pp. 1–16.

Chen, F., Mackey, A.J., Stoeckert, C.J., Jr., and Roos, D.S. (2006). OrthoMCL-DB: Querying a comprehensive multi-species collection of ortholog groups. Nucleic Acids Res. *34*, D363–D368.

Chookajorn, T., Dzikowski, R., Frank, M., Li, F., Jiwani, A.Z., Hartl, D.L., and Deitsch, K.W. (2007). Epigenetic memory at malaria virulence genes. Proc. Natl. Acad. Sci. USA *104*, 899–902.

Cortes, A., Carret, C., Kaneko, O., Lim, B.Y., Ivens, A., and Holder, A.A. (2007). Epigenetic silencing of Plasmodium falciparum genes Linked to erythrocyte invasion. PLoS Pathog. *3*, e107.

Cui, L., Miao, J., Furuya, T., Li, X., Su, X.Z., and Cui, L. (2007). PfGCN5-mediated histone H3 acetylation plays a key role in gene expression in Plasmodium falciparum. Eukaryot. Cell *6*, 1219–1227.

Cui, L., Fan, Q., Cui, L., and Miao, J. (2008). Histone lysine methyltransferases and demethylases in Plasmodium falciparum. Int. J. Parasitol. *38*, 1083–1097.

De Silva, E.K., Gehrke, A.R., Olszewski, K., Leon, I., Chahal, J.S., Bulyk, M.L., and Llinas, M. (2008). Specific DNA-binding by apicomplexan AP2 transcription factors. Proc. Natl. Acad. Sci. USA *105*, 8393–8398.

Duraisingh, M.T., Voss, T.S., Marty, A.J., Duffy, M.F., Good, R.T., Thompson, J.K., Freitas-Junior, L.H., Scherf, A., Crabb, B.S., and Cowman, A.F. (2005). Heterochromatin silencing and locus repositioning linked to regulation of virulence genes in Plasmodium falciparum. Cell *121*, 13–24.

Dzikowski, R., Frank, M., and Deitsch, K. (2006). Mutually exclusive expression of virulence genes by malaria parasites is regulated independently of antigen production. PLoS Pathog. *2*, e22.

Dzikowski, R., Li, F., Amulic, B., Eisberg, A., Frank, M., Patel, S., Wellems, T.E., and Deitsch, K.W. (2007). Mechanisms underlying mutually exclusive expression of virulence genes by malaria parasites. EMBO Rep. *8*, 959–965.

Fernandez, V., Hommel, M., Chen, Q.J., Hagblom, P., and Wahlgren, M. (1999). Small, clonally variant antigens expressed on the surface of the Plasmodium falciparum-infected erythrocyte are encoded by the rif gene family and are the target of human immune responses. J. Exp. Med. *190*, 1393–1403.

Figueiredo, L.M., Pirrit, L.A., and Scherf, A. (2000). Genomic organisation and chromatin structure of Plasmodium falciparum chromosome ends. Mol. Biochem. Parasitol. *106*, 169–174.

Freitas-Junior, L.H., Bottius, E., Pirrit, L.A., Deitsch, K.W., Scheidig, C., Guinet, F., Nehrbass, U., Wellems, T.E., and Scherf, A. (2000). Frequent ectopic recombination of virulence factor genes in telomeric chromosome clusters of P. falciparum. Nature *407*, 1018–1022.

Freitas-Junior, L.H., Hernandez-Rivas, R., Ralph, S.A., Montiel-Condado, D., Ruvalcaba-Salazar, O.K., Rojas-Meza, A.P., Mancio-Silva, L., Leal-Silvestre, R.J., Gontijo, A.M., Shorte, S., and Scherf, A. (2005). Telomeric heterochromatin propagation and histone acetylation control mutually exclusive expression of antigenic variation genes in malaria parasites. Cell *121*, 25–36.

Fried, M., and Duffy, P. (1996). Adherence of Plasmodium falciparum to chondroitin sulfate A in the human placenta. Science *272*, 1502–1504.

Gardner, M.J., Hall, N., Fung, E., White, O., Berriman, M., Hyman, R.W., Carlton, J.M., Pain, A., Nelson, K.E., Bowman, S., et al. (2002). Genome sequence of the human malaria parasite Plasmodium falciparum. Nature *419*, 498–511.

Grewal, S.I., and Jia, S. (2007). Heterochromatin revisited. Nat. Rev. Genet. *8*, 35–46.

Hall, N., Pain, A., Berriman, M., Churcher, C., Harris, B., Harris, D., Mungall, K., Bowman, S., Atkin, R., Baker, S., et al. (2002). Sequence of Plasmodium falciparum chromosomes 1, 3–9 and 13. Nature *419*, 527–531.

Hediger, F., Neumann, F.R., Van Houwe, G., Dubrana, K., and Gasser, S.M. (2002). Live imaging of telomeres: yKu and Sir proteins define redundant telomere-anchoring pathways in yeast. Curr. Biol. *12*, 2076–2089.

Jensen, A.T., Magistrado, P., Sharp, S., Joergensen, L., Lavstsen, T., Chiucchiuini, A., Salanti, A., Vestergaard, L.S., Lusingu, J.P., Hermsen, R., et al. (2004). Plasmodium falciparum associated with severe childhood malaria preferentially expresses PfEMP1 encoded by group A var genes. J. Exp. Med. *199*, 1179–1190.

Kelly, J.M., McRobert, L., and Baker, D.A. (2006). Evidence on the chromosomal location of centromeric DNA in Plasmodium falciparum from etoposide-mediated topoisomerase-II cleavage. Proc. Natl. Acad. Sci. USA *103*, 6706–6711.

Kyes, S.A., Rowe, J.A., Kriek, N., and Newbold, C.I. (1999). Rifins: A second family of clonally variant proteins expressed on the surface of red cells infected with Plasmodium falciparum. Proc. Natl. Acad. Sci. USA *96*, 9333–9338.

Kyes, S.A., Kraemer, S.M., and Smith, J.D. (2007). Antigenic variation in Plasmodium falciparum: Gene organization and regulation of the var multigene family. Eukaryot. Cell *6*, 1511–1520.

Lavazec, C., Sanyal, S., and Templeton, T.J. (2007). Expression switching in the stevor and Pfmc-2TM superfamilies in Plasmodium falciparum. Mol. Microbiol. *64*, 1621–1634.

Lavstsen, T., Salanti, A., Jensen, A.T., Arnot, D.E., and Theander, T.G. (2003). Sub-grouping of Plasmodium falciparum 3D7 var genes based on sequence analysis of coding and non-coding regions. Malar. J. *2*, 27.

Le Roch, K.G., Zhou, Y., Blair, P.L., Grainger, M., Moch, J.K., Haynes, J.D., De La Vega, P., Holder, A.A., Batalov, S., Carucci, D.J., and Winzeler, E.A. (2003). Discovery of gene function by expression profiling of the malaria parasite life cycle. Science *301*, 1503–1508.

Leech, J.H., Barnwell, J.W., Miller, L.H., and Howard, R.J. (1984). Identification of a strain-specific malarial antigen exposed on the surface of Plasmodium falciparum-infected erythrocytes. J. Exp. Med. *159*, 1567–1575.

Lopez-Rubio, J.J., Gontijo, A.M., Nunes, M.C., Issar, N., Hernandez Rivas, R., and Scherf, A. (2007). 5′ flanking region of var genes nucleate histone modification patterns linked to phenotypic inheritance of virulence traits in malaria parasites. Mol. Microbiol. *66*, 1296–1305.

Lunyak, V.V. (2008). Boundaries. Boundaries…Boundaries??? Curr. Opin. Cell Biol. *20*, 281–287.

Mancio-Silva, L., Rojas-Meza, A.P., Vargas, M., Scherf, A., and Hernandez-Rivas, R. (2008). Differential association of Orc1 and Sir2 proteins to telomeric domains in Plasmodium falciparum. J. Cell Sci. *121*, 2046–2053.

Marty, A.J., Thompson, J.K., Duffy, M.F., Voss, T.S., Cowman, A.F., and Crabb, B.S. (2006). Evidence that Plasmodium falciparum chromosome end clusters are cross-linked by protein and are the sites of both virulence gene silencing and activation. Mol. Microbiol. *62*, 72–83.

Merrick, C.J., and Duraisingh, M.T. (2007). Plasmodium falciparum Sir2: An unusual sirtuin with dual histone deacetylase and ADP-ribosyltransferase activity. Eukaryot. Cell. *6*, 2081–2091.

Miao, J., Fan, Q., Cui, L., and Li, J. (2006). The malaria parasite Plasmodium falciparum histones: Organization, expression, and acetylation. Gene *369*, 53–65.

Michishita, E., McCord, R.A., Berber, E., Kioi, M., Padilla-Nash, H., Damian, M., Cheung, P., Kusumoto, R., Kawahara, T.L., Barrett, J.C., et al. (2008). SIRT6 is a histone H3 lysine 9 deacetylase that modulates telomeric chromatin. Nature *452*, 492–496.

Mourier, T., Carret, C., Kyes, S., Christodoulou, Z., Gardner, P.P., Jeffares, D.C., Pinches, R., Barrell, B., Berriman, M., Griffiths-Jones, S., et al. (2008). Genome-wide discovery and verification of novel structured RNAs in Plasmodium falciparum. Genome Res. *18*, 281–292.

Nakayama, J., Rice, J.C., Strahl, B.D., Allis, C.D., and Grewal, S.I. (2001). Role of histone H3 lysine 9 methylation in epigenetic control of heterochromatin assembly. Science *292*, 110–113.

Nunes, M.C., Goldring, J.P., Doerig, C., and Scherf, A. (2007). A novel protein kinase family in Plasmodium falciparum is differentially transcribed and secreted to various cellular compartments of the host cell. Mol. Microbiol. *63*, 391–403.

Ralph, S.A., Scheidig-Benatar, C., and Scherf, A. (2005). Antigenic variation in Plasmodium falciparum is associated with movement of var loci between subnuclear locations. Proc. Natl. Acad. Sci. USA *102*, 5414–5419.

Scherf, A., Hernandez-Rivas, R., Buffet, P., Bottius, E., Benatar, C., Pouvelle, B., Gysin, J., and Lanzer, M. (1998). Antigenic variation in malaria: in situ switching, relaxed and mutually exclusive transcription of var genes during intra-erythrocytic development in Plasmodium falciparum. EMBO J. *17*, 5418–5426.

Scherf, A., Lopez-Rubio, J.J., and Riviere, L. (2008a). Antigenic Variation in Plasmodium falciparum. Annu. Rev. Microbiol. *62*, 445–470.

Scherf, A., Riviere, L., and Lopez-Rubio, J.J. (2008b). SnapShot: var gene expression in the malaria parasite. Cell *134*, 190.

Shankaranarayana, G.D., Motamedi, M.R., Moazed, D., and Grewal, S.I. (2003). Sir2 regulates histone H3 lysine 9 methylation and heterochromatin assembly in fission yeast. Curr. Biol. *13*, 1240–1246.

Snow, R.W., Guerra, C.A., Noor, A.M., Myint, H.Y., and Hay, S.I. (2005). The global distribution of clinical episodes of Plasmodium falciparum malaria. Nature *434*, 214–217.

Stubbs, J., Simpson, K.M., Triglia, T., Plouffe, D., Tonkin, C.J., Duraisingh, M.T., Maier, A.G., Winzeler, E.A., and Cowman, A.F. (2005). Molecular mechanism for switching of P. falciparum invasion pathways into human erythrocytes. Science *309*, 1384–1387.

Taddei, A., Van Houwe, G., Hediger, F., Kalck, V., Cubizolles, F., Schober, H., and Gasser, S.M. (2006). Nuclear pore association confers optimal expression levels for an inducible yeast gene. Nature *441*, 774–778.

Tonkin, C.J., van Dooren, G.G., Spurck, T.P., Struck, N.S., Good, R.T., Handman, E., Cowman, A.F., and McFadden, G.I. (2004). Localization of organellar proteins in Plasmodium falciparum using a novel set of transfection vectors and a new immunofluorescence fixation method. Mol. Biochem. Parasitol. *137*, 13–21.

Voss, T.S., Healer, J., Marty, A.J., Duffy, M.F., Thompson, J.K., Beeson, J.G., Reeder, J.C., Crabb, B.S., and Cowman, A.F. (2006). A var gene promoter controls allelic exclusion of virulence genes in Plasmodium falciparum malaria. Nature *439*, 1004–1008.

Yamada, T., Fischle, W., Sugiyama, T., Allis, C.D., and Grewal, S.I. (2005). The nucleation and maintenance of heterochromatin by a histone deacetylase in fission yeast. Mol. Cell *20*, 173–185.